

## Supplementary Information

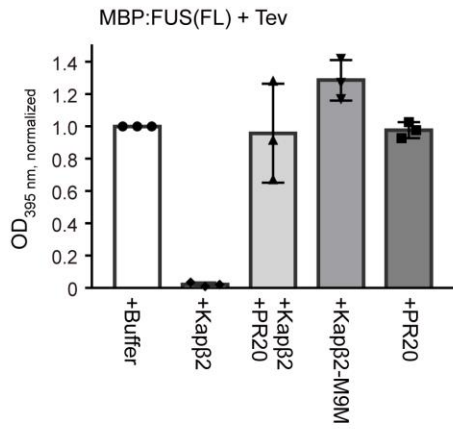
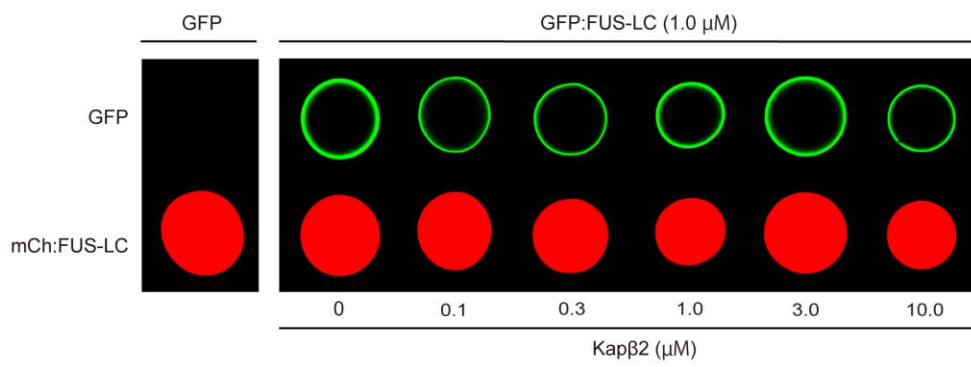
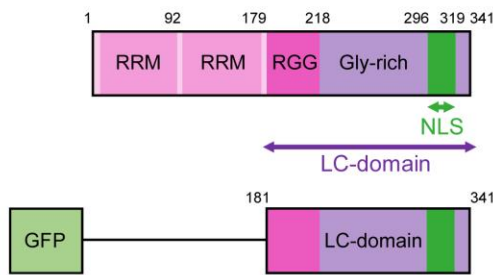
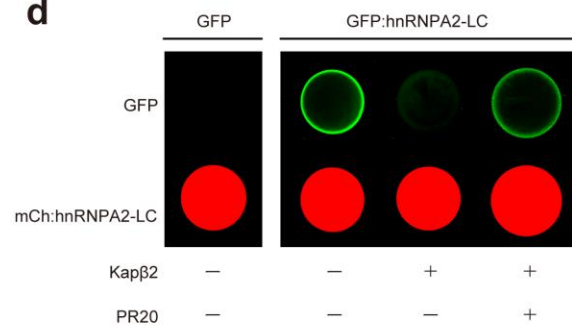
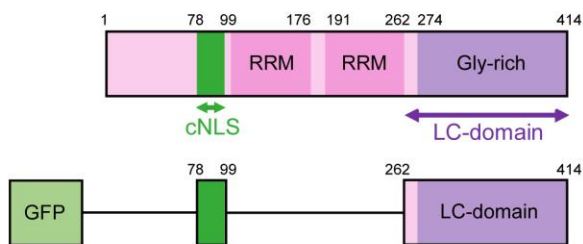
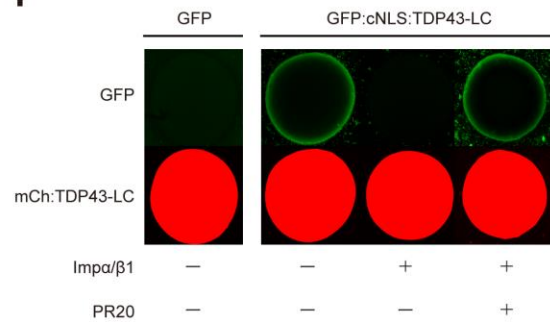
### ***C9orf72*-derived arginine-rich poly-dipeptides impede phase modifiers**

Hitoki Nanaura<sup>1</sup>, Honoka Kawamukai<sup>1</sup>, Ayano Fujiwara<sup>1</sup>, Takeru Uehara, Yuichiro Aiba, Mari Nakanishi, Tomo Shiota, Masaki Hibino, Pattama Wiriyasermkul, Sotaro Kikuchi, Riko Nagata, Masaya Matsubayashi, Yoichi Shinkai, Tatsuya Niwa, Taro Mannen, Naritaka Morikawa, Naohiko Iguchi, Takao Kiriyama, Ken Morishima, Rintaro Inoue, Masaaki Sugiyama, Takashi Oda, Noriyuki Kodera, Sachiko Toma-Fukai, Mamoru Sato, Hideki Taguchi, Shushi Nagamori, Osami Shoji, Koichiro Ishimori, Hiroyoshi Matsumura, Kazuma Sugie, Tomohide Saio\*, Takuya Yoshizawa\*, Eiichiro Mori\*

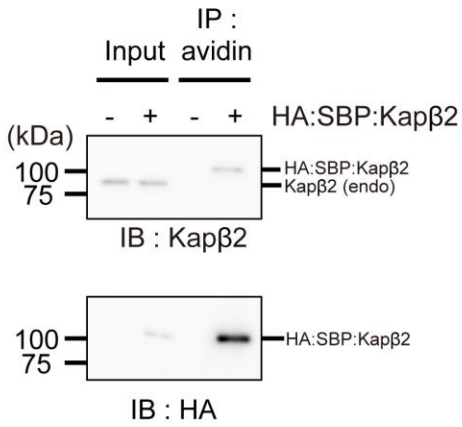
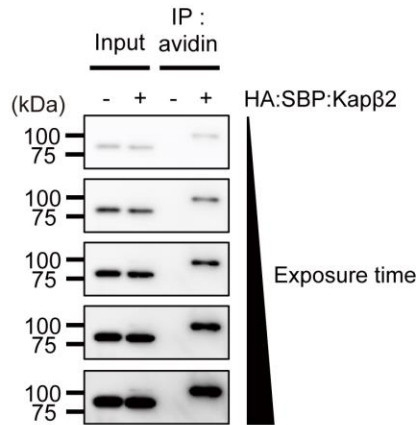
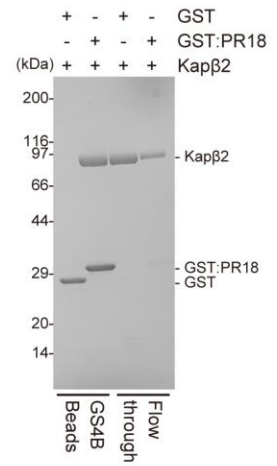
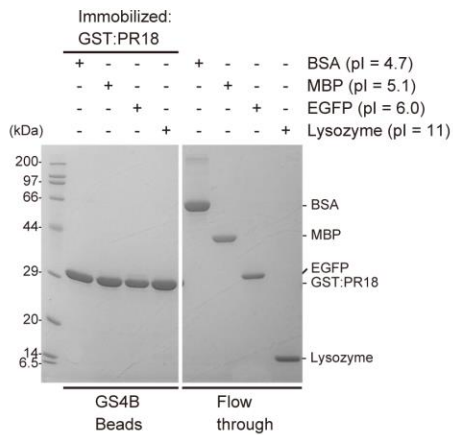
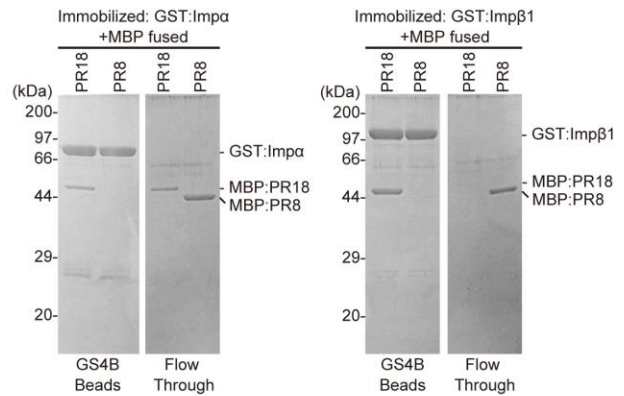
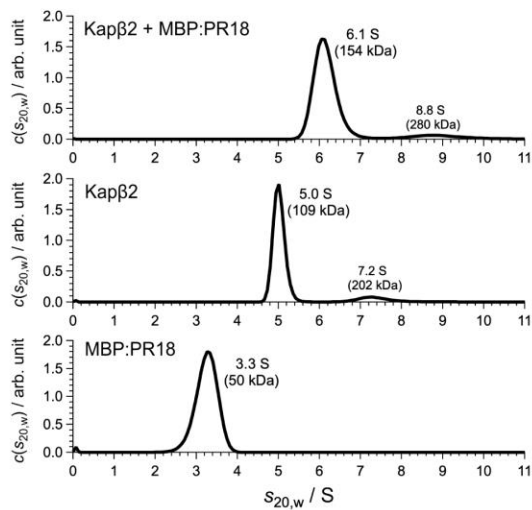
<sup>1</sup>These authors contributed equally: Hitoki Nanaura, Honoka Kawamukai, Ayano Fujiwara.

\*Corresponding authors.

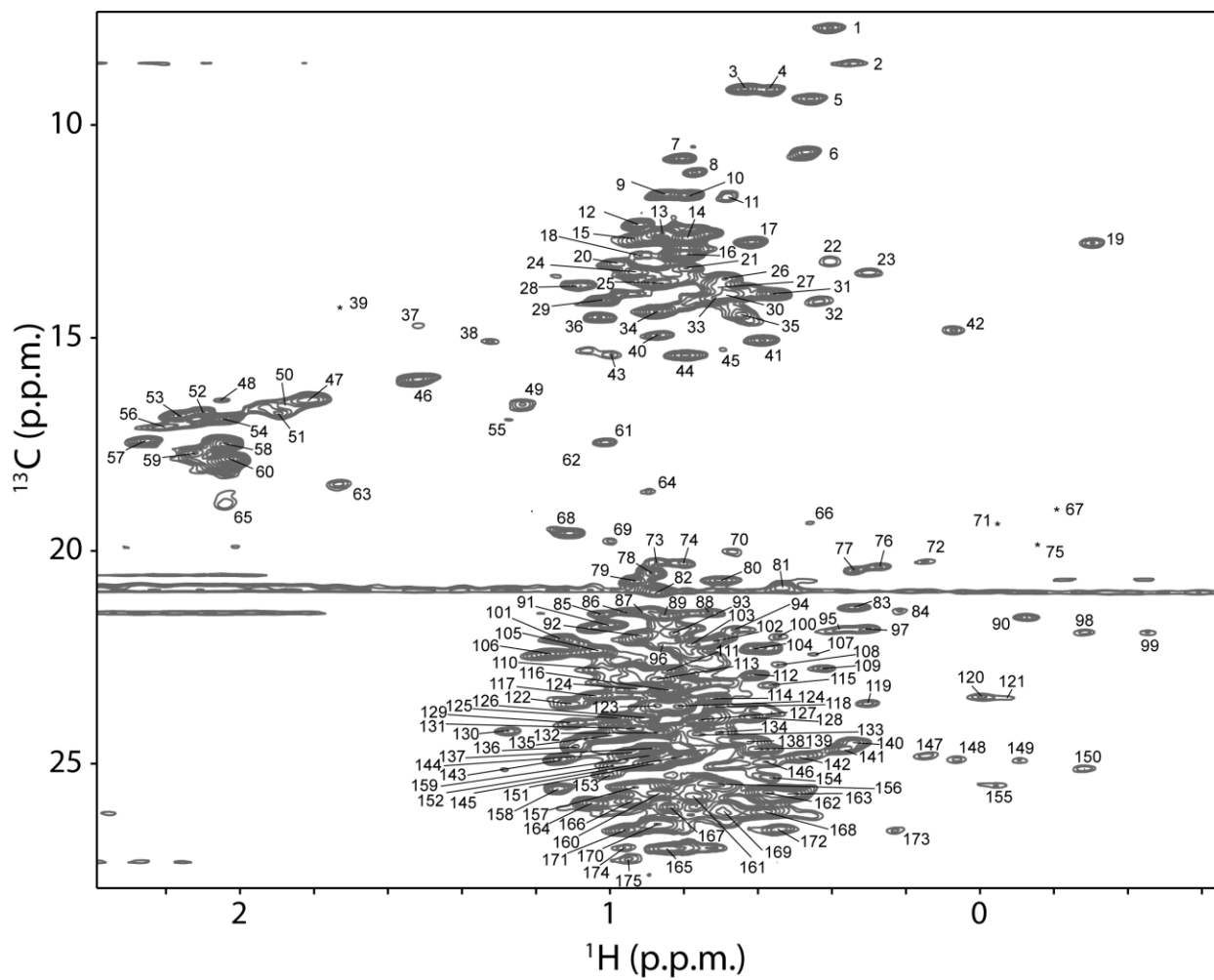
E-mail: saio@tokushima-u.ac.jp, t-yosh@fc.ritsumei.ac.jp, emori@naramed-u.ac.jp.

**a****b****c****d****e****f**

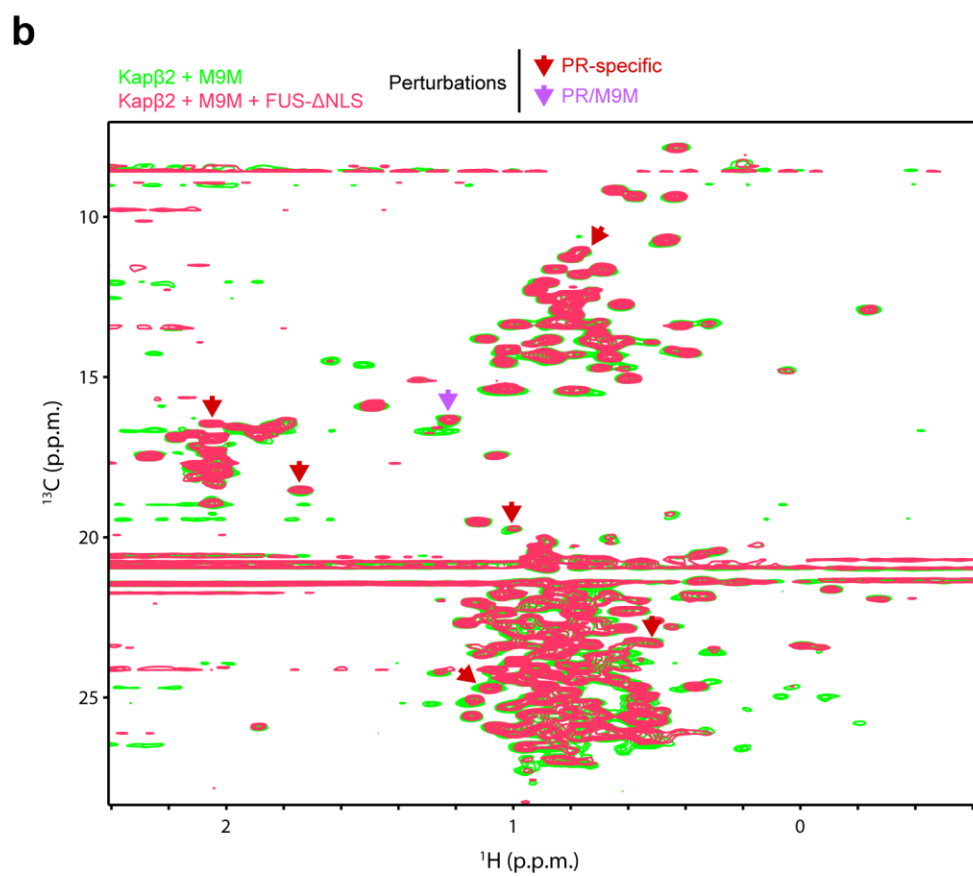
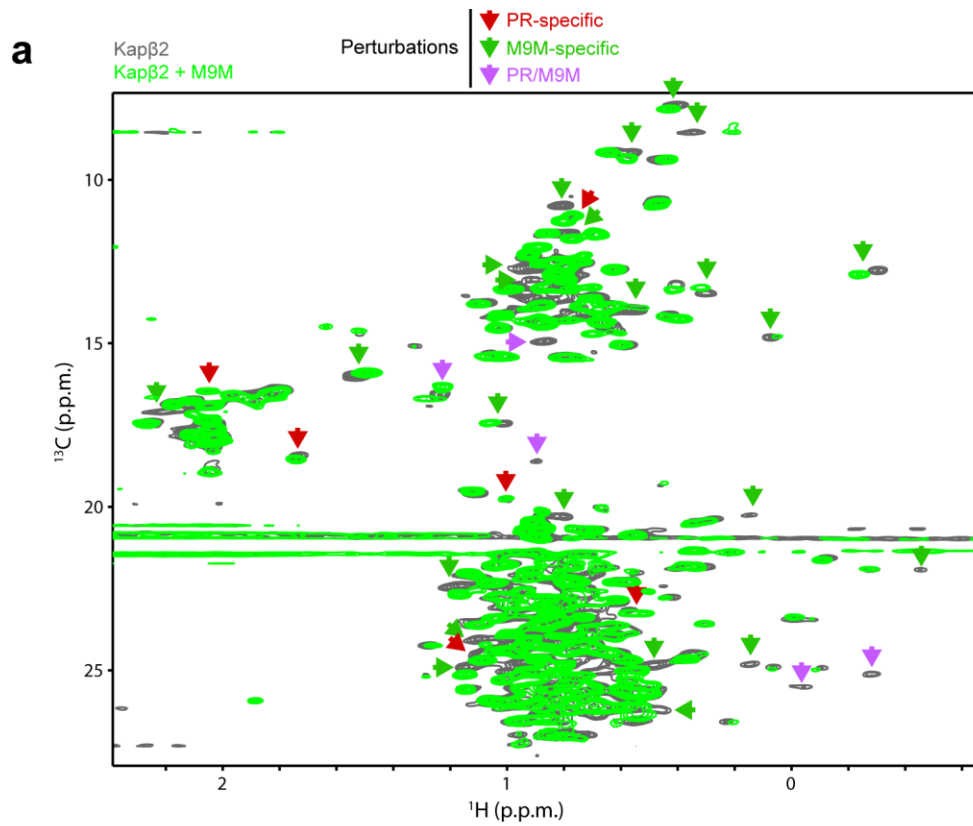
**Supplementary Fig. 1. Domain architecture and hydrogel binding assay of RNA binding proteins.** **a)** Turbidity of 8  $\mu\text{M}$  MBP:FUS in the presence of buffer,  $\pm$  8  $\mu\text{M}$  Kap $\beta$ 2,  $\pm$  8  $\mu\text{M}$  Kap $\beta$ 2-M9M complex, and  $\pm$  8  $\mu\text{M}$  PR20. OD 395 nm is normalized to measurement of MBP:FUS + buffer + Tev. Mean of three technical replicates,  $\pm$ SD. **b)** Hydrogel droplets of mCh:FUS-LC (lower images) were incubated with 1.0  $\mu\text{M}$  of GFP (left panel) or 1.0  $\mu\text{M}$  of GFP:FUS-LC (right panel) and visualized by confocal microscopy. GFP:FUS-LC was challenged for homotypic polymer extension in the presence of different concentration of Kap $\beta$ 2 (left to right: 0.1  $\mu\text{M}$ , 0.3  $\mu\text{M}$ , 1.0  $\mu\text{M}$ , 3.0  $\mu\text{M}$ , 10.0  $\mu\text{M}$ , respectively). **c)** Domain architecture of hnRNPA2 and GFP fusion hnRNPA2-LC (GFP:hnRNPA2-LC). NLS of hnRNPA2 (residue 296-319) is located in the middle of LC-domain. **d)** mCh:hnRNPA2-LC (lower images) were incubated with 1.0  $\mu\text{M}$  of GFP (left panel) or 1.0  $\mu\text{M}$  of GFP:hnRNPA2-LC (right panel). GFP:hnRNPA2-LC containing Kap $\beta$ 2 (1.0  $\mu\text{M}$ ) was challenged in the absence or presence of PR20 (1.0  $\mu\text{M}$ ). **e)** Domain architecture of TDP43 and GFP-tagged cNLS fusion TDP43-LC (GFP:cNLS:TDP43-LC). **f)** mCh:TDP43-LC (lower images) were incubated with 1.0  $\mu\text{M}$  of GFP (left panel) or 1.0  $\mu\text{M}$  of GFP:cNLS:TDP43-LC (right panel) in the absence or presence of Imp $\alpha/\beta$ 1 (1.0  $\mu\text{M}$ /1.0  $\mu\text{M}$ ) and/or PR20 (1.0  $\mu\text{M}$ ). Source data are provided as a Source Data file. RGG: Arg-Gly-Gly motif, RRM: RNA Recognition Motif, ZnF: zinc-finger domain.

**a****b****c****d****e****f**

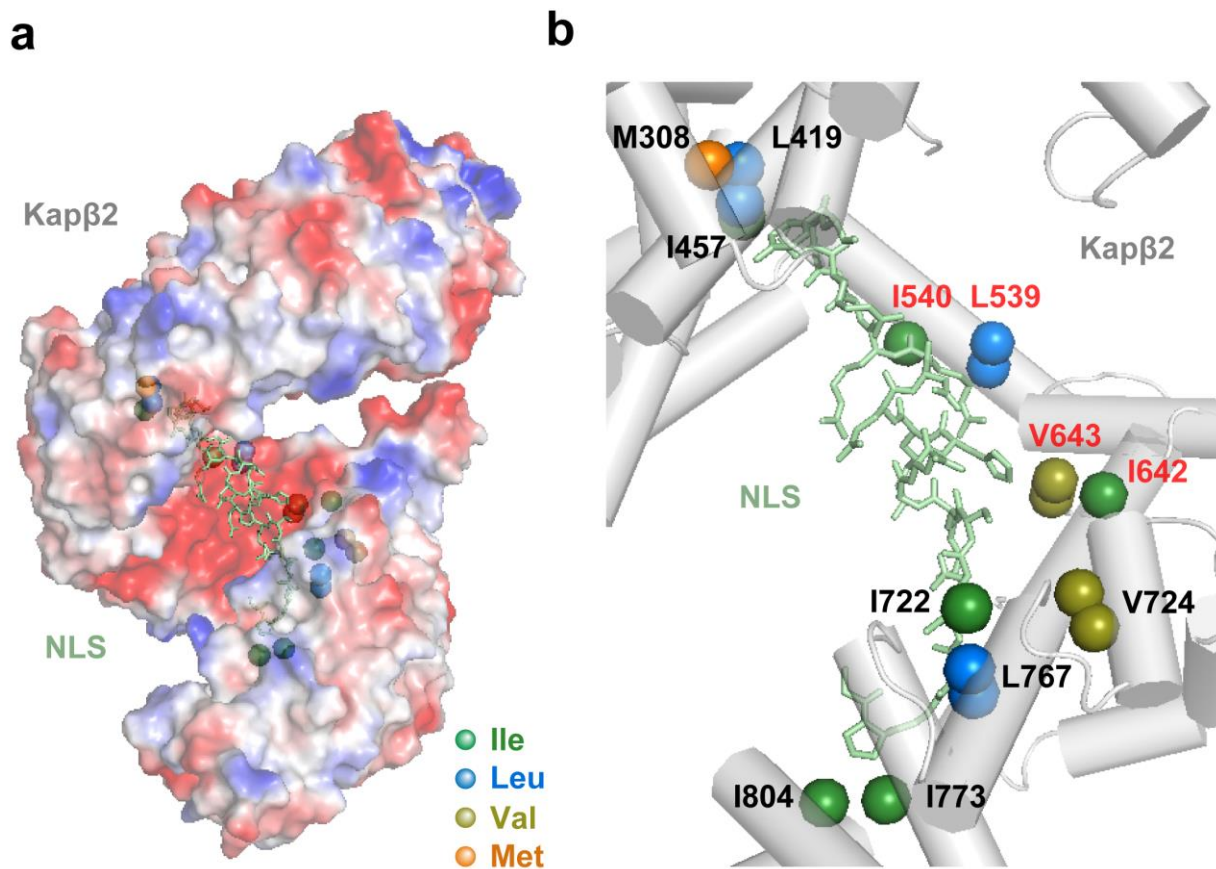
**Supplementary Fig. 2. Interaction between nuclear import receptors and PR poly-dipeptides.** **a-b)** Immunoprecipitation showing the recognition of endogenous and exogenous Kap $\beta$ 2 by anti-Kap $\beta$ 2 antibody. **c)** Pull-down binding assay showing interaction between GST:PR18 and Kap $\beta$ 2. **d)** Pull-down binding assay showing no interaction between GST:PR18 and proteins, BSA, MBP, EGFP, and Lysozyme. **e)** Pull-down binding assay showing interaction between MBP:PR18 with GST:Importin $\alpha$  or GST:Importin $\beta$ 1. **f)** Analytical ultracentrifugation showing complex formation between Kap $\beta$ 2 and MBP:PR18. The experiments (**a**, **c**, **e**) were independently repeated two or three times with similar results. Source data are provided as a Source Data file.



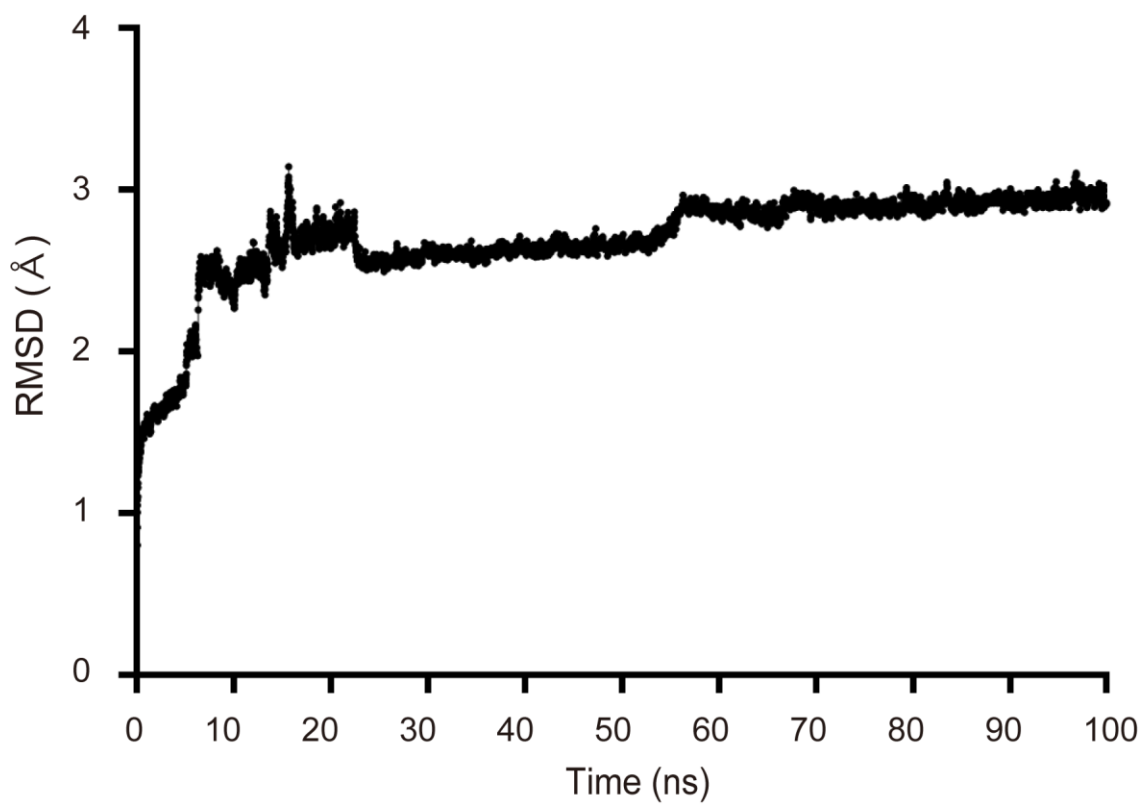
**Supplementary Fig. 3. Solution NMR of Kap $\beta$ 2.**  $^1\text{H}$ - $^{13}\text{C}$ -correlated methyl NMR spectra of [U- $^2\text{H}$ ; Ile-1- $^{13}\text{CH}_3$ ; Leu, Val- $^{13}\text{CH}_3/^{12}\text{CH}_3$ ]-labeled Kap $\beta$ 2. The peaks are labeled with peak numbers. Asterisks indicate the positions of the small peaks that were absent in the threshold setting of the figure.



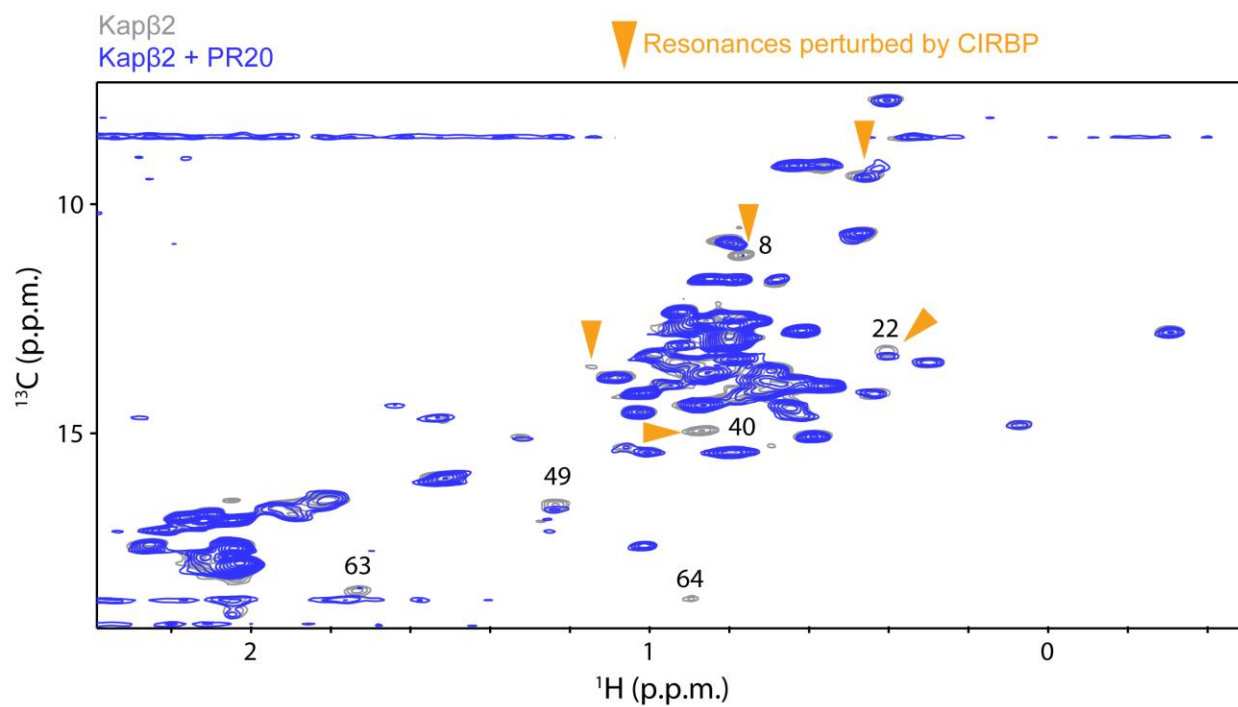
**Supplementary Fig. 4. Interaction between Kap $\beta$ 2 and M9M/FUS- $\Delta$ NLS investigated by solution NMR.** **a)**  $^1\text{H}$ - $^{13}\text{C}$ -correlated methyl NMR spectra of [ $\text{U}$ - $^2\text{H}$ ; Ile-1- $^{13}\text{CH}_3$ ; Leu, Val- $^{13}\text{CH}_3/\text{C}^2\text{H}_3$ ]-labeled Kap $\beta$ 2 (grey) and that in complex with M9M (green). The significant perturbations were observed, which is consistent with the high affinity between Kap $\beta$ 2 and M9M as reported in a previous study (Supplementary Table 1). **b)**  $^1\text{H}$ - $^{13}\text{C}$ -correlated methyl NMR spectra of [ $\text{U}$ - $^2\text{H}$ ; Ile-1- $^{13}\text{CH}_3$ ; Leu, Val- $^{13}\text{CH}_3/^{12}\text{CH}_3$ ]-labeled Kap $\beta$ 2 in complex with M9M, in the absence (green) and presence (magenta) of FUS- $\Delta$ NLS. Significant representative perturbations are indicated by arrows. Perturbations only seen for PR20 are indicated by red arrows. Perturbations only seen for M9M are indicated by green arrows. Perturbations common to PR20 and M9M are indicated by the purple arrows. Perturbed resonances induced by the addition of FUS- $\Delta$ NLS were distinct from those induced by PR20.



**Supplementary Fig. 5. Structural model of Kap $\beta$ 2 and NLS of FUS.** **a)** Electrostatic surface potential of Kap $\beta$ 2 (4FDD). Positive and negative surface potentials are drawn in blue and red, respectively. The methyl groups of isoleucine, leucine, valine, and methionine residues located close to the Kap $\beta$ 2 cavity are represented as spheres colored green, blue, yellow, and orange, respectively. **b)** An expanded view of Kap $\beta$ 2 cavity. Methyl groups of isoleucine, leucine, valine, and methionine are represented as spheres colored green, blue, yellow, and orange, respectively. L539, I540, V643, and I642 are located on negatively charged cavity. NLS of FUS is represented as a stick model, colored pale green. The structure was drawn using PyMol program.



**Supplementary Fig. 6. RMSD values of all atoms from the reference structure (0 ns) for MD simulation.** Root-mean-square deviations (RMSDs) of all atoms were plotted as a function of time for the 100-ns MD simulation (Fig. 5a, b) of Kap $\beta$ 2 and PR poly-dipeptides. Source data are provided as a Source Data file.



**Supplementary Fig. 7. Comparison of NMR perturbations of Kapβ2 induced by PR20 and CIRBP-RGG.**  $^1\text{H}$ - $^{13}\text{C}$ -correlated methyl NMR spectra of [U- $^2\text{H}$ ; Ile-1- $^{13}\text{CH}_3$ ; Leu, Val- $^{13}\text{CH}_3/\text{C}^2\text{H}_3$ ]-labeled Kapβ2 in the absence (grey) and presence (blue) of PR20. The resonances that showed significant perturbations by interaction with CIRBP-RGG<sup>1</sup> are indicated by arrowheads.

**Supplementary Table 1. Kd value against Kap $\beta$ 2 determined by ITC**

Ligand	Tag	Kd (nM)	Reference	Buffer
PR18	MBP	81.3	This work	20 mM HEPES pH7.4, 150 mM NaCl, 10% glycerol, 2 mM bME
FUS(475-526)	MBP	31	Gonzalez et al., Sci Rep, 2021	20 mM Tris-HCl pH7.4, 150 mM NaCl, 10% Glycerol, 2 mM bME
FUS(453-500)	MBP	6000	Gonzalez et al., Sci Rep, 2021	20 mM Tris-HCl pH7.4, 150 mM NaCl, 10% Glycerol, 2 mM bME
FUS(371-500)	MBP	170	Gonzalez et al., Sci Rep, 2021	20 mM Tris-HCl pH7.4, 150 mM NaCl, 10% Glycerol, 2 mM bME
FUS(1-500)	MBP	160	Gonzalez et al., Sci Rep, 2021	20 mM Tris-HCl pH7.4, 150 mM NaCl, 10% Glycerol, 2 mM bME
FUS(415-460)	MBP	No binding	Gonzalez et al., Sci Rep, 2021	20 mM Tris-HCl pH7.4, 150 mM NaCl, 10% Glycerol, 2 mM bME
FUS(371-452)	MBP	4000	Gonzalez et al., Sci Rep, 2021	20 mM Tris-HCl pH7.4, 150 mM NaCl, 10% Glycerol, 2 mM bME
FUS(278-385)	MBP	No binding	Gonzalez et al., Sci Rep, 2021	20 mM Tris-HCl pH7.4, 150 mM NaCl, 10% Glycerol, 2 mM bME
FUS(1-370)	MBP	35000	Gonzalez et al., Sci Rep, 2021	20 mM Tris-HCl pH7.4, 150 mM NaCl, 10% Glycerol, 2 mM bME
FUS(476-526)	MBP	71.5	Yoshizawa et al., Cell, 2018	20 mM HEPES pH7.4, 150 mM NaCl, 10% glycerol, 2 mM bME
FUS(453-526)	MBP	173	Yoshizawa et al., Cell, 2018	20 mM HEPES pH7.4, 150 mM NaCl, 10% glycerol, 2 mM bME
FUS(371-526)	MBP	209	Yoshizawa et al., Cell, 2018	20 mM HEPES pH7.4, 150 mM NaCl, 10% glycerol, 2 mM bME
FUS(1-526)	MBP	158.7	Yoshizawa et al., Cell, 2018	20 mM HEPES pH7.4, 150 mM NaCl, 10% glycerol, 2 mM bME
M9NLS(A1, 257-305)	MBP	42	Lee et al., Cell, 2006	20 mM Tris pH7.5, 100 mM NaCl, 2 mM bME
hnRNP M(41-70)	MBP	10	Cansizoglu et al., NSMB, 2007	20 mM Tris pH7.5, 100 mM NaCl, 2 mM bME
M9M	MBP	0.107	Cansizoglu et al., NSMB, 2007	20 mM Tris pH7.5, 100 mM NaCl, 2 mM bME
FUS(454-526)	–	600	Dormann et al., EMBO J, 2012	20 mM sodium phosphate buffer pH6.8, 50 mM NaCl, 1 mM EDTA, 1 mM DTT
FUS(489-526)	–	2800	Dormann et al., EMBO J, 2012	20 mM sodium phosphate buffer pH6.8, 50 mM NaCl, 1 mM EDTA, 1 mM DTT
FUS(504-526)	–	20000	Dormann et al., EMBO J, 2012	20 mM sodium phosphate buffer pH6.8, 50 mM NaCl, 1 mM EDTA, 1 mM DTT
FUS(473-503)	–	11700	Dormann et al., EMBO J, 2012	20 mM sodium phosphate buffer pH6.8, 50 mM NaCl, 1 mM EDTA, 1 mM DTT



### **Supplementary References**

1. Bourgeois B, *et al.* Nonclassical nuclear localization signals mediate nuclear import of CIRBP. *Proc Natl Acad Sci USA* **117**, 8503-8514 (2020).